

**2010 NDIA GROUND VEHICLE SYSTEMS ENGINEERING AND TECHNOLOGY SYMPOSIUM
MODELING & SIMULATION, TESTING AND VALIDATION (MSTV) MINI-SYMPOSIUM
AUGUST 17-19 DEARBORN, MICHIGAN**

MULTI-RESOLUTION RAPID PROTOTYPING OF VEHICLE COOLING SYSTEMS

Jean-Jacques Malosse, PhD
Computational Sciences, LLC
Madison, AL

Maciej Z. Pindera, PhD
Computational Sciences, LLC
Madison, AL

Yuzhi Sun, PhD
Steven R. Vosen, PhD
Computational Sciences, LLC
Madison, AL

ABSTRACT

This paper describes a work in progress on the development of general, Open Architecture multi-resolution software for rapid prototyping and analysis of complex systems using a Co-simulation approach. Although the approach can be used for rapid analysis of a wide class of complex physical systems, the current focus of this work is on the modeling of the engine cooling system in the Ford Escape Hybrid SUV vehicle. The paper discusses two aspects of this work: development of the co-simulation environment, development of models of the cooling system components with focus on the A/C system using the R134a refrigerant. The major component models are based on dimensional reduction of the 3D Navier-Stokes equations. The resulting 1D equations are subsequently partitioned along the axial direction resulting in systems of 0D non-linear ordinary differential equations. The equations are then solved using a very efficient approach using Chebyshev polynomials. We also present preliminary results on component response to variations in selected system parameters.

INTRODUCTION

Many physical systems can be of sufficient complexity (both geometric and physics-related) to make fully resolved 3D simulations impractical due to complicated gridding requirements and potentially very slow execution times on complex grids. Moreover, a single software package may not have all the capabilities required for complete vehicle thermal analysis. Modern army and commercial vehicles with hybrid power systems that contain multiple heat-generating and rejection components is one example of such systems, as shown in Fig. 1. This particular system shows three independent but coupled cooling loops: engine, motor-electronics (M/E) module and the battery pack using the A/C system.

The distributed multi-resolution approach sidesteps these difficulties by: a) partitioning a complex system into interacting components that can be represented by reduced models of varying levels of fidelity; and b) using several codes in coupled parallel or parallel/series execution, each performing a set of specific computational tasks and exchanging information in real time. For generality, information exchange takes place with the aid of a

simulation environment that allows inclusion of additional system component models and legacy codes with minimal code modifications. Such a computing approach is also known as *grid*, or *co-simulation*. The examples discussed in this paper show the advantages of this approach for analysis of complex systems

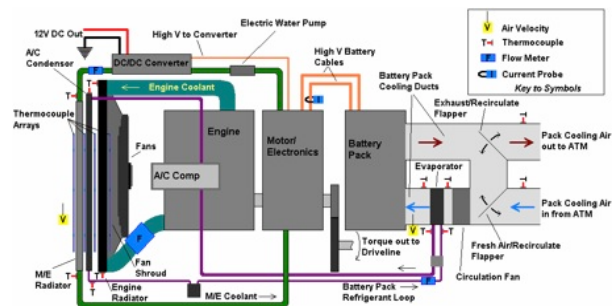


Figure 1: Multi-component Cooling System in a Ford Escape Hybrid

The availability of efficient, rapid prototyping software is especially important in design of thermal management

strategies in modern vehicles with conventional and hybrid power systems, sensor/control modules, and electric propulsion units, as Fig. 1 indicates. These electronic systems are not only significant sources of heat, but may also operate in harsh thermal-mechanical conditions (e.g., in the engine compartment). Analysis of the components' internals, determining their placement, and predictions of system-level thermal performance is a complex multi-physics problem and investigation of different cooling strategies during the design phase therefore can be very expensive and time-intensive using conventional simulation approaches. On the other hand, the multi-resolution co-simulation methods allow the use of the time-intensive, high-fidelity models only where needed, with the rest of the system being modeled using much faster, lower resolution approaches.

MULTI-RESOLUTION ANALYSIS

Multi-resolution analysis partitions a complex continuous system into components where each component is represented by a separate model. In our approach we have developed a general wrapper routine that encapsulates a large class of such models as stand-alone codes, with communication interfaces that allow the codes to exchange data with one another between suitably defined boundary and/or volume conditions. This approach allows simulation of a large class of dynamic systems to different levels of accuracy since it allows coupling of models defined on 1D, 2D or 3D domains. Data exchange is brokered by the Open Architecture, co-simulation environment *CoSim* that connects the system components. Fig. 2 shows the connection scheme for a stand-alone A/C system.

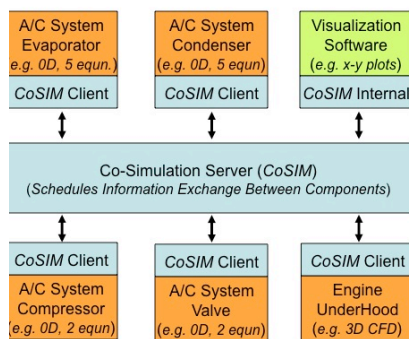


Figure 2: CoSim-Brokered A/C Connection Scheme

The 0D component models are connected to a 3D CFD model that calculates the under-hood ambient conditions that regulate heat exchange between the system and the environment. As indicated, *CoSim* also allows visualization of a component response history during run time. The main advantage of connecting the system components through an

independent environment rather than connecting them directly is that additional components can be added to the system without affecting the original connectivity or data transfer synchronization.

Although system partitioning is by necessity problem specific, the possibility of using separate codes to simulate the dynamics of different components gives this form of multi-resolution approach a large degree of latitude in how the systems are partitioned. Multi-resolution analysis can be carried out on different levels and with different requirements which may be, for example:

1. Fully-resolved: full 3D analysis performed on the vehicle-package system using standard CFD.
2. Mixed-resolution: combination of full 2D or 3D detailed/meshed model and reduced-order representations of components within the system.
3. System-level: assembly of reduced-order models of components for rapid generation of results for the entire vehicle-package system.
4. Interface with legacy codes: each code performs a different analysis task. For example, one code can generate vehicle surface heat flux data (due to internal heating) that another code will use to compute vehicle surface cooling and thermal signature.
5. Selective focusing: using reduced-order models (with increased resolution) on specific components/assemblies, while using regular reduced-order models for the remaining components. This feature allows fast analyses of parametric changes in the 'focused' portions, and is extremely useful for rapid thermal prototyping, signature management, and optimization.

Simulation Environment and Data Exchange

The basic function of the simulation environment is to schedule data transfer between the different codes that comprise the system of interest. The codes do not communicate directly, but only through the environment. The environment also contains transformer functions that can be used for data scaling, rescaling, and modeling of components, and contains a user-expandable library of component models of different fidelities, common to vehicle cooling systems. The environment structure allows an arbitrary number of codes to be connected in an arbitrary fashion, and exchange an arbitrary amount and type of data. Data exchange is executed using the CORBA communications protocol allowing platform-to-platform data exchange over a computer network. The protocols are encapsulated in a set of Application Programming

Interfaces (APIs). APIs are codelets designed to be appended to any stand-alone component code, with minimum modification to the host codes. Corresponding APIs exist in *CoSim*. Fig. 3 shows a schematic of the data exchange process.

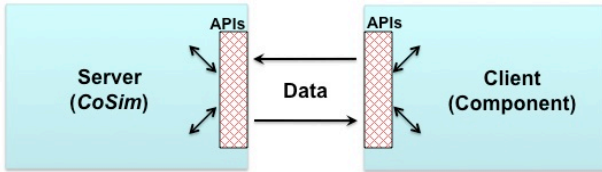


Figure 3: Server-Client connectivity Between the *CoSim* Environment and System Component Models.

The environment executes the following functions:

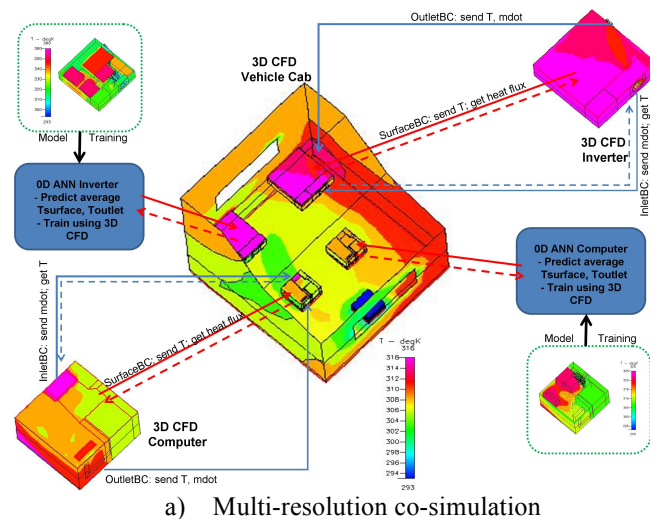
1. Data reception and reception scheduling (using APIs);
2. Data distribution and sequencing to proper models;
3. Data pre-processing (mainly appropriate scaling operations);
4. Data processing (if library models are used in simulations);
5. Data post-processing (appropriate output rescaling);
6. Data transmission and transmission scheduling (using APIs).

Data is exchanged at a rate specified by the user. Any data can be exchanged (pressure, temperature, etc.) from any point in the computational domain. The user is responsible for providing the software front-ends that will extract (impose) the required data from (to) the code of interest and supply the data to the APIs for transmission (or reception). When component models use implicit solvers, information is typically passed every several iterations to make the simulation tightly coupled. During the multi-component, multi-resolution simulation, the environment ensures that the executions of each code and data exchange are properly synchronized.

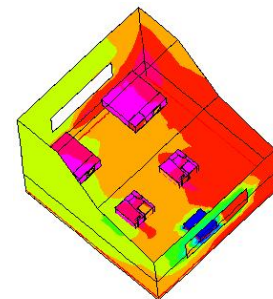
Fig. 4 shows an example of the principle applied to a multi resolution simulation of heating of a prototypical vehicle cab by electronics components. The system components consist of a 3D CFD-based vehicle cab and CFD models of a computer and an inverter. Additional components include reduced models of a computer and an inverter modeled by Artificial Neural Networks (ANNs). The computer and inverter models generate heat that is transferred to the cab interior through the walls and the internal cooling fans. Cooling air is taken into the components from the cab interior, is heated by internal heat-generating components, and is subsequently exhausted

back into the cab at elevated temperatures. In this example the cab and the components are gridded separately. The cab contains surface-gridded placeholder domains that exchange boundary heat information with the component models as shown.

This example illustrates another feature of the approach in that it allows complex simulations that would not otherwise be possible to do with some commercial codes. Boundary conditions at the cooling fan inlets of the components require mass flow (or velocity) and temperature information. While the mass flow/velocity can be specified as constant, there is no simple way of specifying the inlet temperature since it is a part of the solution. Depending on the code, use of User Routines is one possible approach. The coupled co-simulation approach treats this difficulty in a natural manner, since all the fields used by each of the components are specified exactly. In this case, the inlet temperature to the components is obtained from the solution on the cab-level.



a) Multi-resolution co-simulation



b) Whole-field CFD simulation

Figure 4: Distributed Multi-Resolution Simulation of Heating Inside a Vehicle Cab, (Pindera, 2009)

The results indicate that the temperature fields predicted by the two simulation approaches do not vary by more than

5K. The difference in simulation run times can be considerable, however, and scales directly with the reduction in the number of computational cells used in CFD simulations, when some of the sub-domains are replaced by reduced models.

APPLICATION to COOLING VEHICLE SYSTEMS

In this section we discuss applications to the analysis of cooling systems in conventional and hybrid power vehicles.

Cooling of a Conventional Diesel Power-Plant

Fig. 5 shows a schematic of a prototypical cooling system of a mid-sized Army truck. The dashed line indicated models that comprise a reduced system: engine, radiator, transmission oil cooler, and transmission.

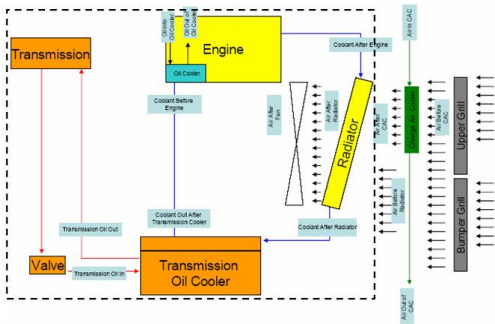


Figure 5: Schematic based on TARDEC Document “Tactical Vehicle M&S Data”

The complete engine cooling system can be represented by six basic modules composed of nine interconnected elements as indicated in the Table below.

Table 1. Components Available for Representation of Engine Cooling System

Component	Internal Sub-Models	Function
Engine	<ul style="list-style-type: none"> Power plant Engine oil cooler 	Heat generator
Transmission oil cooler	<ul style="list-style-type: none"> Heat rejection from trans. oil, Heat absorption by engine coolant 	Heat exchanger
Pump	<ul style="list-style-type: none"> Pressure head CFD flow 	Mass flow calculation
Radiator	<ul style="list-style-type: none"> Heat rejection from coolant 	Heat exchanger
Transmission	<ul style="list-style-type: none"> Heat addition to engine coolant 	Heat generator

The components can be graphically connected as shown in Fig. 6 using a GUI developed for co-simulation applications of this type.

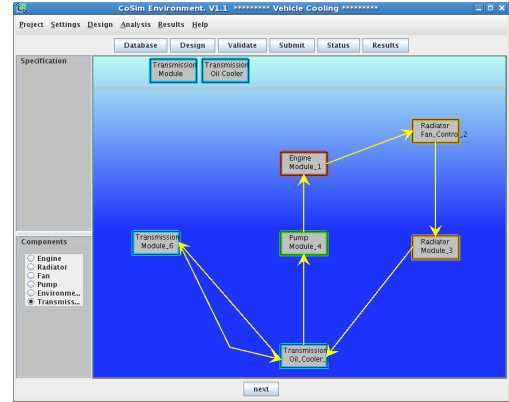


Figure 6: Basic Cooling System Connectivity of the Component Modules.

As indicated in Fig. 5, the system uses five directly connected reduced models of: engine, radiator, transmission oil cooler, transmission and coolant pump. Although other components such as piping, junctions, and other elements are not directly taken into account, they can be easily added into the overall connection scheme. We have also added a simple (PI) controller module to automatically regulate the coolant temperature through radiator output, for example the fan speed.

For this particular configuration, the coolant exists in one phase only and the various components can be modeled by a simple lumped parameter approach shown by the energy flow schematic in Fig. 7.

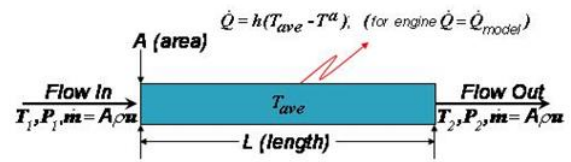


Figure 7: Basic Model of Heat Exchange Systems

The energy flow into the system is provided from other connected components and the energy flow out of the system is provided to other connected components. For the components of interest the flow is assumed incompressible, the flow rate \dot{m} does not vary in the heat transfer components and is set by the pressure model. For simplicity, flow inside these components currently does not have pressure losses, and so inlet and outlet pressures are the same, or $P_{in} = P_{out}$. This is not a limitation of our approach – merely a simplifying component assumption that could be relaxed if needed. Heat transfer rate \dot{Q} is modeled as a Newton-type process where:

$$\dot{Q} = h(T_{ave} - T^0); \quad h = \text{heat transfer coefficient}$$

Eq. 2 gives the rate of change of outlet temperature T2 in terms of the inlet area, characteristic length, density, specific heat, inlet temperature and heat flux (heating or cooling) as denoted by $(A, L, \rho, c_p, T_1, \dot{Q})$, respectively.

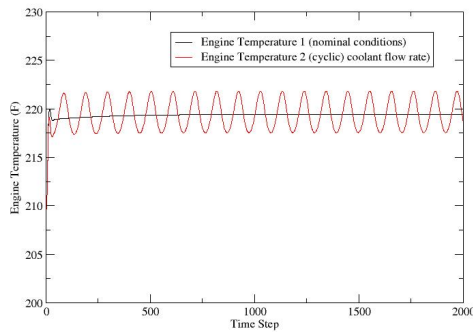
$$AL\rho c_p \frac{dT_2}{dt} = -\rho u A c_p (T_2 - T_1) + h(T^a - T_{ave})$$

Assuming that, and $T_{ave} = (T_1 + T_2)/2$; $\dot{m} = A\rho u$, the solution to the above takes on a simple form:

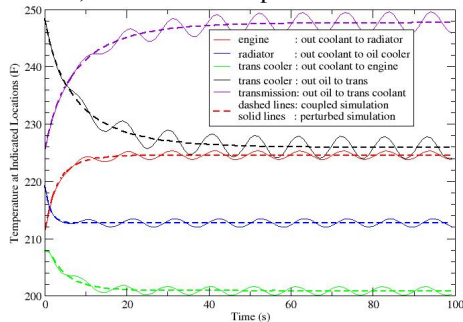
$$T_2 = (T_2^o - c)e^{-at} + c; \quad c = aT_1 - \frac{h(T_1 - T^a)}{\dot{m}c_p + h/2}; \quad b = aT_1 - \frac{h(T_1 - T^a)}{AL\rho c_p}$$

Model parameters a and b were estimated from steady state data experimental for each component. Heat generated by the engine was calculated using a universal correlation of diesel engine performance developed by Gloverk (1994a, b), which relates engine speed and torque to the fuel consumption. Given the amount of fuel burned and fuel efficiency, we use the correlation to estimate the amount of heat that must be removed from the engine through cooling.

Fig. 8 shows typical dynamic system response of the various components to perturbations in the engine coolant mass flow rate, heat fluxes at the transmission oil cooler



a) Mass flow rate perturbations



b) Transmission cooler heat flux perturbations

Figure 8: Effect of Cyclic Perturbations of Selected Variables on the System Response

Fig. 9 shows the engine temperature results for controller tasked with adjusting the radiator output required for keeping the engine temperature at a desired (constant) level when engine heat production increases. For simplicity, instead of using the power plant model, we ramped up the generated heat by 50% over nominal, over 100 time steps. The controller uses a simple Proportional-Integral strategy to vary the rejected heat in the radiator in order to maintain the desired engine temperature.

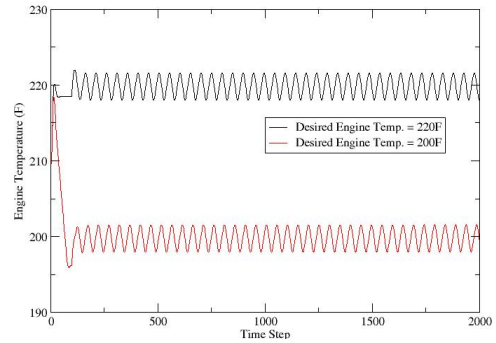


Figure 9: Radiator Control for Off-nominal Engine Operations

The target temperatures were set at the nominal 220F and at 255F. Fig. 9 shows that the radiator operations can be adjusted so that the engine temperatures can attain desired levels. The temperature response is oscillatory since in this simulation the optimized adjusts the radiator operations dynamically, during the course of operations/simulations.

Cooling of a Hybrid Gasoline Engine Power-Plant

Hybrid systems are considerably more difficult to model and analyze since they can contain several separate, coupled cooling loops. Fig. 1 shows a typical system used in a Ford Escape Hybrid that contains the engine, motor-electronics (M/E) module and the battery pack cooling that is tied to the A/C system. Since the latter contains two-phase coolant flow, component models of the type shown in Fig. 7 are not adequate, and more sophisticated component models are required. In this section we discuss the work-in-progress on modeling of the main components of the A/C system: evaporator and condenser.

Fig. 10 shows the flow physics in the evaporator and condenser. The models are based on the work of Rasmussen (2002) and Shah (2003). Flow in both components is assumed to be one dimensional, with no pressure drop. In the evaporator, the fluid is assumed to enter the evaporator in a mixture of liquid and gas, and exits as a gas only (overheat region). The variables describing the evaporator dynamics are: length of the two-phase region; spatially uniform pressure; outlet temperature, and wall temperatures in each region. Our

model does not yet handle the cases where the fluid enters the evaporator as a sub-cooled liquid, or exits as a two-phase mixture.

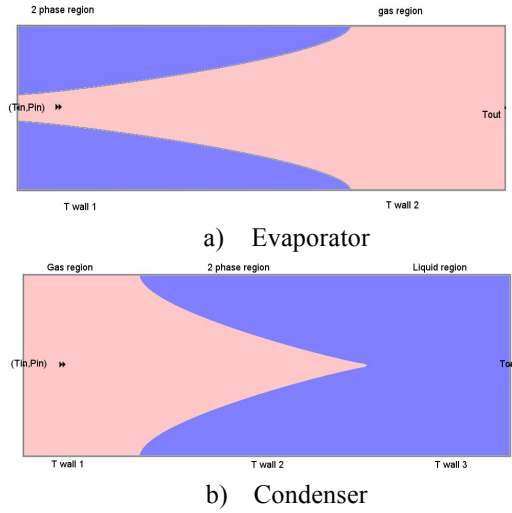


Figure 10: Flow Physics in the Two Main A/C Components

In the condenser, we assume that the fluid enters as a gas and exits as a liquid. In this model, we add two extra system variables: length of the liquid columns and the wall temperature of the liquid region.

Evaporator Model

Below we summarize the derivation of the evaporator model. The condenser is derived in an analogous manner. The derivation is based on a reduction of one-dimensional Navier-Stokes mass and energy conservation equations to their equivalent 0D, lumped parameter form defined by a system of ordinary differential equations (ODEs). Momentum conservation is not used since we assume no pressure drop in the device.

The evaporator is divided into two separate regions: two-phase, and pure gas. The physical properties are taken as invariant in each region. The model consists of six independent equations.

1&2: Mass conservation in the single and two-phase regions.

$$\frac{\partial \rho}{\partial t} + \frac{\partial(\rho u)}{\partial z} = 0$$

3&4: Energy conservation in the single and two-phase regions. We perform an energy balance between the energy transferred through the wall by conduction and the decrease in internal energy.

$$\frac{\partial(\rho A_{cs} h - A_{cs} \rho)}{\partial t} + \frac{\partial(\dot{m} h)}{\partial z} = p_i \alpha_i (T_{w1} - T_r)$$

5&6: Energy conservation in the wall in the single and two-phase regions.

$$(c_p \rho A) \frac{\partial T_w}{\partial t} = p_i \alpha_i (T_r - T_w) + p_o \alpha_o (T_a - T_w)$$

The lumped parameter ODEs are obtained by integrating the 1D Navier-Stokes equations along the length of the component, in the different regions of interest. The two mass conservation equations are combined to result in the final transient formulation given in terms five equations for (region length, pressure, outlet temperature, and wall temperatures in the two regions). The details are given in Rasmussen (2002). The model can be expressed in the matrix form

$$Z(X)X = F(X) \quad (1)$$

where

$$X = \begin{bmatrix} L_1 \\ P \\ T_{out} \\ T_{w1} \\ T_{w2} \end{bmatrix}; F = \begin{bmatrix} f_1 \\ f_2 \\ f_3 \\ f_4 \\ f_5 \end{bmatrix}; Z = \begin{bmatrix} z_{11} & 0 & 0 & 0 & 0 \\ z_{21} & z_{22} & z_{23} & 0 & 0 \\ z_{31} & z_{32} & z_{33} & 0 & 0 \\ 0 & 0 & 0 & z_{44} & 0 \\ 0 & 0 & 0 & 0 & z_{55} \end{bmatrix}$$

The coolant was taken to be 1,1,1,2-Tetrafluoroethane (R134a). Its temperature and density dependent thermodynamic coefficients were evaluated using the correlations developed by Astina and Sato (2004). The temperature dependent transport coefficients were evaluated using the correlations developed by Kraus et al. (1993) and Yata et al. (2005).

Numerical Solution

The above system can be written in the form $\dot{X} = G(X, t)$. We assume that the function G is *analytic*, and also assume that the initial system state at $t = 0$ is represented by the vector X_0 . From the Picard–Lindelöf theorem, the above differential equation has a unique solution. Consequently, the future behavior of the model will be determined by its initial state. Furthermore, the function $X(t)$ is analytical in t and therefore, this function can be represented by an infinite series. The above equation is not linear and we will linearize it to simplify its solution.

Linearization Scheme

Given the initial state X_0 , we advance the solution by a small timestep T . Then, the function $X(t)$ will remain close to X_0 and we may write

$$X(t) = X_0 + \delta X(t)$$

where $\delta X(t)$ is small compared to X_0 . We assume that during a small timestep, $G(X,t) = G(X)$ does not depend on time. Let $G'(X_0)$ be the Jacobian matrix of G . We assume that the order 2 correction will be small. The differential equation we solve then becomes:

$$(\dot{X}_0 + \delta \dot{X}) = \dot{X} = G(X) = G(\dot{X}_0 + \delta X) \approx G(X_0) + G'(X_0)\delta X$$

Expanding and solving for $\delta \dot{X}$ yields

$$\delta \dot{X} = G(X_0) + G'(X_0)\delta X$$

The above equation is of the matrix form $\dot{X} = AX + b$ where A and b are constant, with the solution of the form

$$X(t) = X_0 + E(t)b; \quad E(t) = \int_0^t e^{A(t-\tau)} d\tau = \left[\int_0^t e^{-A\tau} d\tau \right] e^{At}$$

The matrix exponential is defined as convergent series for any matrix A and any parameter t , $e^{At} = \sum_{n \in \mathbb{N}} A^n t^n / n!$.

Instead of expressing the above series in the usual power basis $(1, t, t^2, \dots)$, we express the series in the modified Chebychev polynomials basis. The Chebychev polynomials are defined by as follows:

$$T_0(x) = 1; \quad T_1(x) = x; \quad T_n(x) = 2xT_{n-1}(x) - T_{n-2}(x)$$

Remark: Another definition of Chebychev polynomials that shows close relationship Fourier series is:

$$T_n(x) = \cos(n \cos^{-1}(x))$$

After performing a scaling, we now define the modified Chebychev polynomials in a more convenient form, as

$$T_n(t) = T_n\left(\frac{2t - T}{T}\right)$$

We note that for $n \geq 1$, the highest degree term of $T_n(x)$ will be 2^{n-1} . Therefore, we can approximate the function e^{At} with a lower degree polynomial if we express the infinite series in modified Chebychev polynomials compared to power polynomials. This true as well for $E(t)$. This result is also a consequence of Neumann's theorem (Davies, 1975).

Even if e^{At} is a convergent series, the explicit calculation of this series requires some caution because the terms that we add and subtract can become very large. We perform the calculation by interpolating. Let N be a degree such that the truncated Chebychev series of e^{At} at degree N can represent the latter at a given tolerance. Then, the explicit truncated Chebychev series can be represented within this tolerance by *interpolating* the function e^{At} at the N roots of the modified Chebychev polynomial T_N (Malosse, 1992). We compute the interpolating matrices e^{At_i} at the roots t_i of the modified Chebychev polynomial T_n by induction since

$$e^{At_{i+1}} = e^{A(t_{i+1}-t_i+t_i)} = e^{At_i} \times e^{A(t_{i+1}-t_i)}$$

and therefore we are dealing with much smaller matrices:

$A(t_{i+1} - t_i)$ with $t_{i+1} - t_i = T$. When the function e^{At} has been expressed explicitly in the Chebychev polynomials basis, the numerical calculation of its integral $E(t)$ is straightforward. The computation of the exponential e^{At} where M is any matrix is performed recursively by noting that $e^{2M} = (e^M)^2$. One of the advantages of using Chebychev series over Runge-Kutta methods is that we obtain *explicit parametric functions* instead of point-like functions.

Asymptotic Behavior

We first assume that $\dot{m}_{in} = \dot{m}_{out}$. In this configuration, the physical system will converge to equilibrium and therefore, the eigenvalues $\lambda_k + i\mu_k$ of A will be such that $\lambda_k \leq 0$. For these conditions we can prove that as $t \rightarrow \infty$, $e^{At} \rightarrow M$ where M is a constant matrix.

When $\dot{m}_{in} \neq \dot{m}_{out}$, the system cannot converge. For example, if $\dot{m}_{in} - \dot{m}_{out} < 0$, the mass of the fluid will eventually become negative. Therefore, the mass flow imbalance can only be *transient*.

As the system reaches equilibrium, the vector derivative \dot{X} vanishes and the right hand side of Eq. 1 becomes zero. Noting that as the term f_3 also vanishes, the system becomes underdetermined since it contains *four equations with five unknowns*. Such an underdetermined system can contain in principle an infinite number of possible equilibrium states. We are currently extending the formulation to account for this behavior. However,

numerical experiments indicate that in many situations this effect may not be large.

Numerical Experiments

We have performed quasi-transient numerical experiments to evaluate the model behavior under perturbations of the mass flow rate and the outside temperature, under equilibrium mass flow rate. We chose the system pressure, outlet temperature, and the length of the two-phase region as the representative system variables.

Fig. 11 shows the evaporator response to step-function variations in the mass flow rate in the range 0.0009-0.001 kg/s. The total tube length is 43 cm.

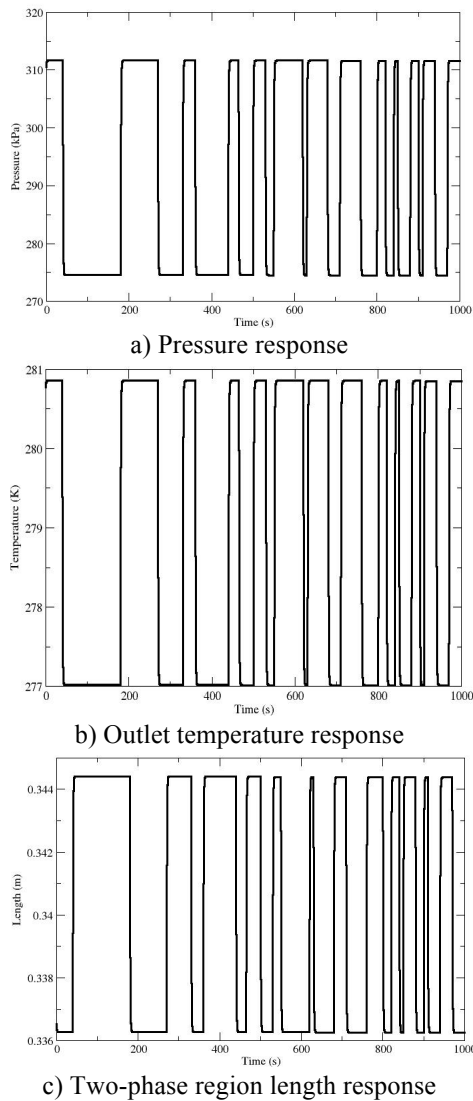


Figure 11: Evaporator response to mass flow perturbations

The geometry and run conditions were based on the work of Shah (2003), where similar results were reported in his Fig. 4.23. For a 10% variation in the mass flow-rate Shah reports variation in the pressure in the range 274-311 kPa. Our result is consistent with this data. The outlet fluid temperature varies by plus or minus 5 degrees when the air temperature varies by plus or minus 5 degrees as well. We note that the length of the two-phase region varies by plus or minus 1 cm.

Fig. 12 shows the evaporator response to step-function variations in the outside air temperature in the range 305-310 K.

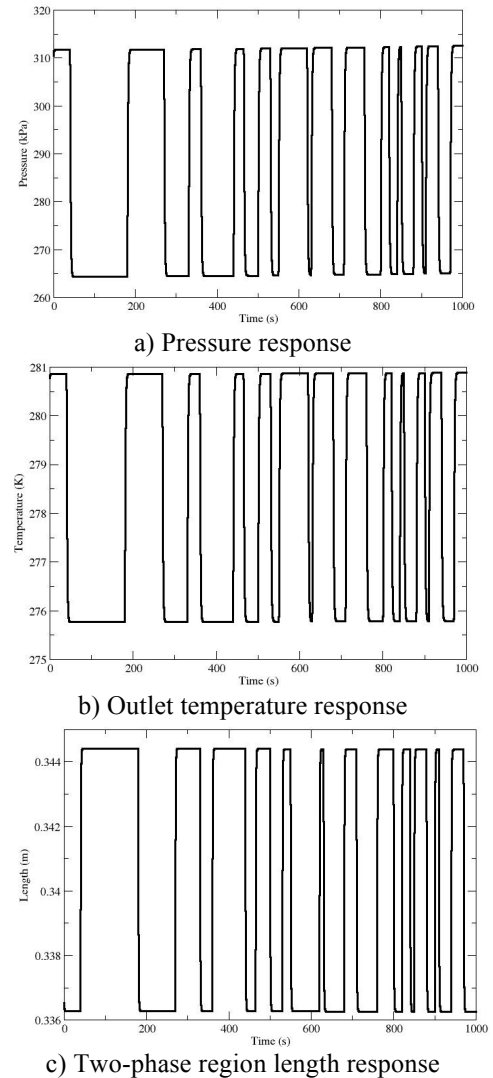


Figure 12: Evaporator response to ambient temperature perturbations

We note a degree of hysteresis in the variation of the two-phase length zone. The total measured hysteresis is in the order of 1 mm for 25 steps. This variation per time step is relatively small, approximately 40 microns per 1cm, or 0.4%. As we mentioned above, for given mass flows and a given outside air temperature, the system has an *infinite number of possible equilibriums*. Since the differential equations we solve are non linear, nothing guarantees that the system will return to its previous equilibrium state. This demonstrates that the evaporator model is incomplete.

In this model, we note that the length of the two-phase region increases with time. Since this region becomes larger, we expect that the quantity of liquid will become larger and therefore, the mixing ratio will vary. In our model (derived from Rasmussen, 2002) we assume that the mixing ratio is constant. At this time, we are developing a model that removes the time-independence restriction of the mixing ratio.

The next step is to connect the four components of the A/C system (evaporator, compressor, condenser, expansion valve) and perform scoping simulations of component and system-level performance. We will subsequently combine the A/C system with the engine and M/E module cooling systems (Fig. 1) and embed the major heat transfer components (e.g. radiators and the evaporator) in the under-hood, CFD-based domain, as was done in the simulations shown in Fig. 4. The models will be based on the components used in the Ford Escape Hybrid, and simulation results will be compared to the experimental data that we have generated for the Escape.

NOMENCLATURE

<i>Variables names</i>	<i>Indices</i>
A: Tube area	1: first region
A_{cs} : tube cross section	2: second region
α : heat transfer coefficient	a: outside air
C_p : specific heat capacity at constant pressure	f: liquid
γ_m : mixing ratio	g: gas
h: specific enthalpy	i: tube interior
L: length	in: inlet
\dot{m} : mass flow rate	o: tube exterior
P: pressure	out: outlet
ρ : density	r: refrigerant
T: temperature	w: wall
V: volume	

SUMMARY AND CONCLUSIONS

Simulation-based prototyping of complex systems can be very challenging in terms of domain grid complexity, density and the associated long simulation times. A

practical alternative is to partition such systems into interacting component models of desired resolution and fidelity and couple the execution of these models into an integrated computational scheme. The resultant multi-resolution co-simulations can provide an optimum balance between desired accuracy, simulation times, and computational resources. Moreover, interchanging component models of different resolution allows one to selectively focus-in on the details of their operation, in the context of whole-system dynamics. This approach is of particular importance in the virtual, simulation-based prototyping of thermal management strategies for complex cooling systems embedded in vehicle under-the-hood systems for which the use of full CFD analysis is impractical.

The first two examples showed the accuracy, speed and the stability of the multi-resolution approach. In general, the acceleration of execution times compared to full CFD analysis is due to lower number of computational cells resulting from replacement of fully gridded system components by equivalent reduced models. Execution of even complex reduced models such as those associated with the A/C system can be timed in terms of milliseconds; in comparison to their gridded equivalents, the computational time spent in execution of such models is therefore essentially insignificant. For modern vehicles with multiple heat generating components, the multi-resolution approach can thus be the enabling methodology for performing system-level thermal management prototyping simulations.

ACKNOWLEDGMENTS

This research is being performed under the Army TACOM SBIR Phase II Project “Co-Simulation Software For Rapid Prototyping Of Vehicle Cooling Systems”, Contract Number W56HZV-09-C-0056. We wish to thank Ms. Mary Goryca, the Program Manager for this project, for developing our interest in hybrid vehicles.

REFERENCES

Astina, I. Made and Sato, H, (2004), “Fundamental equation of state for 1,1,1,2-tetrafluoroethane with an intermolecular potential energy background and reliable ideal-gas properties”, Fluid Phase Equilibria 221 (2004).
 Davies, P.J., (1975), “Interpolation and Approximation”, Dover.
 Krauss, R., Luettmmer-Strathmann, J., Sengers, J.V., and Stephan, K., (1993), “Transport Properties of 1,1,1,2-Tetrafluoroethane (R 134a)”, Int. J. of Thermophysics, 14:4.
 Malosse, J-J., (1992), “Parametrization of Implicit Elliptic Curves by Rational Functions”, Proceedings of the 5th

- IMA Conference on the Mathematics of Surfaces. Edinburgh, 1992.
- Pindera, M.Z. (2009), "Multiresolution Thermal Design/Signature Management Tools For Vehicle Electronics Packages," Phase II Final Report; Army Contract Number: W56HZV-06-C-0571.
- Rasmussen B.P. (2002), "*Control oriented modeling of transcritical vapor compression systems*", M.S Thesis, University of Illinois at Urbana-Champaign, 2002.
- Shah, R. (2003), "*Dynamic Modeling and Control of Single and Multi-Evaporator Subcritical Vapor Compression Systems*", M.S. Thesis, University of Illinois at Urbana-Champaign.
- Vosen, S.R., (2008), "Co-Simulation Software For Rapid Prototyping Of Vehicle Cooling Systems", Final Report Army SBIR Phase I Contract W56HZV-08-C-0088.
- Yata, J., Ueda, Y., and Horis, M., (2005), "*Equations for the Thermal Conductivity of R-32, R-125, R-134a, and R-143a*", Int. J. of Thermophysics, **26**:5, Sept.